SUPPORTING DOCUMENT

Incongruent HIV and tuberculosis co-dynamics in Kenya: Interacting epidemics monitor each other

María S. Sánchez, James O. Lloyd-Smith, Brian G. Williams, Travis C. Porco, Sadie J. Ryan, Martien W. Borgdorff, John Mansoer, Christopher Dye and Wayne M. Getz

TB-HIV Data

We used a total of 106 data points representing different measures collected at various time points and presented in the WHO Global TB Database and the WHO 2001 through 2006 Global Reports. The different types of measures we used are:

1) TB incidence per 100,000 persons per year (per 100K/yr) for 1990, 1995-2004[1];

2) smear-positive TB incidence per 100K/yr for 1990, 1995-2004[1];

3) TB incidence excluding HIV-infected persons (HIV+) per 100K/yr for 1990[1];

4) TB incidence in HIV+ per 100K/yr for 1995-2004[1];

5) smear-positive TB incidence in HIV+ per 100K/yr for 1995-2004[1];

6) TB case notification rates per 100K/yr for 1980, 1981, 1983, 1985-2004[2];

7) smear-positive TB case notification rates per 100K/yr for 1993-2004[1];

8) TB deaths per 100K/yr for 1990, 1995-2004[1];

9) TB deaths excluding HIV+ per 100K/yr for 1990[1];

10) TB deaths in HIV+ per 100K/yr for 1995-2004[1];

11) proportion of cases that are HIV+ in 1999[3], 2000[4], 2001[5], 2002[6], 2003[7], and 2004[2].

Because our model operates on a monthly time step, we summed over our predicted 12 month model outputs to obtain the yearly estimates used to match the observed data points. We assigned an equal weight to all the 106 measures in order to minimize the assumptions we made throughout the study, although it is expected that certain measures and years may be more reliable than others. We originally included an additional 22

prevalence measures in our calibration. We opted to exclude them from the final calibration because these estimates require further assumptions in their calculation, and when included the resulting fit to the preferred measures of case notification, incidence and mortality became substantially worse.

Model Structure

Basic TB model

The following TB model structure description incorporates elements from Salomon *et al*.[8] Our model accounted for the most relevant complexities of TB aetiology, clinical presentations, sociology, and treatment options.[9-11] Moreover, the course of the disease could be vastly different in HIV-infected persons as compared to non-immunocompromised individuals: in most persons TB remains a latent infection and has little effect on their health, but in immunocompromised persons TB infections are likely to become active, and potentially deadly.[12-14]

More specifically (Fig. S1A), susceptible persons could become infected with TB upon contact with infected persons, at a rate given by the force of infection $c_j\lambda$, which varies across HIV stages (with j = 1 corresponding to HIV uninfected, and j = 2-5 corresponding to HIV stages I-IV). This force was calculated at each time step from the current number of persons in a TB infectious category (see below, Model Formulation). We assumed the population mixed at random with density-independent contact rates, so transmission was frequency-dependent. Untreated persons with smear-positive active disease were the most likely to infect others (β_P), followed by the untreated smear-negative (β_N). Smear-positive persons that failed treatment were partially infectious (β_{PF}),

and all other categories were not considered to transmit at measurable rates. Latent slow progressors and recovered individuals became reinfected at a reduced rate as compared to TB naïve persons (b_j<1).

When infected, a person entered a latent slow (with probability p_{Sj}) or a fast latent category (with probability 1-p_{Sj}). Persons in the fast latent stage progressed rapidly to active disease at rate ϕ_{Sj}, while those in the slow latent stage had a reduced endogenous reactivation rate ϕ_{Fj}. Upon development of active TB, a fraction s_{Pj} of persons presented smear positive symptoms, and a fraction 1- s_{Pj} presented smear negative symptoms. Individuals infected with HIV, particularly in the advanced stages, were more likely to be smear-negative due to their reduced immunity.[12,15] Smear-negative persons converted to smear-positive at rate σ_j. A fraction d of persons with active TB, regardless of their smear category, entered the detectable compartment, and a fraction 1-d the non-detectable compartment. This partition represented any kind of impediment to initiating treatment, such as subclinical symptoms or lack of access to health care due to long distance from the home to a TB clinic, social stigma associated with TB infection, financial trouble due to loss of work days while treated, case-finding effort on behalf of the local health services, etc.[16-20] The distinction between smear positive and smear negative cases was retained throughout those compartments categorizing cases that were either active, on treatment, or partially cured, in order to provide flexibility in accounting for any differences in infectiousness, detectability, response to treatment, relapse, etc. Active cases recovered spontaneously without treatment and entered the slow latent compartment at rate π_j.

At each time step cases moved from the detectable category into treatment according to the case-detection rate (θ_j), and then entered a DOTS (with probability t_P for smear-positive and t_N for smear negative) or a non-DOTS program (with corresponding probabilities 1-t_P and 1-t_N). The model was flexible regarding treatment duration, and in this particular study we were investigating treatment durations of 6 months for standard DOTS and 8 months for standard non-DOTS. Patients defaulted at each time step with a certain probability δ_m, or took their medication throughout the entire course. Upon default or completion persons either (1) failed treatment and returned directly to the active category (with probabilities q_{PDj} for smear-positive persons on DOTS, q_{PNj} for smear-positive persons on non-DOTS, q_{NDj} for smear-negative persons on DOTS, q_{NNj} for smear-negative persons on non-DOTS, or $q_{complete,j}$), (2) entered a transiently recovered smear-positive (partially infectious) or smear-negative (non-infectious) category (with corresponding probabilities to (1) above $v_{kl,j}$ or $v_{complete,j}$), or (3) if finished treatment completely recovered in which case they were non-infectious (with probability $s_{complete,j} = 1 - v_{complete,j} - q_{complete,j}$). Transiently recovered persons relapsed back to active at rate ρ_j, and entered the detectable and non-detectable compartments corresponding to their smear status according to the same proportions as originally defined for those progressing to active from the latent stages. As in Salomon *et al.*[8], we did not track treatment history explicitly or modeled distinct retreatment regimens. Persons that completely recovered were assumed to be partially immune to reinfection. All categories suffered the same natural background mortality (μ), and active untreated and treated cases suffer TB associated mortality to varying degrees across HIV stages (μ_{Pj}, μ_{Nj}, $\mu_{PD,j}$, $\mu_{PN,j}$, $\mu_{ND,j}$, $\mu_{NN,j}$).

Basic HIV model

The impact of TB on the epidemiology of HIV is not as substantial as that of HIV on TB.[21-23] Thus, we did not model HIV transmission dynamics explicitly, but incorporated it into the model as an exogenous input using a defined incidence recruitment process that generated historical HIV prevalence patterns. We opted to use those patterns reported most recently for Kenya by Cheluget *et al*.[24], which consist of an increasing trend to 10-11% prevalence in 1997-98, followed by a decline to a present level of approximately 6.7% (Fig. S2 and Fig. 3 in Cheluget *et al.* 2006[24]).

Upon infection with HIV, persons progressed through the 4 HIV disease stages defined by the World Health Organization (Fig. S1B) according to the following time lines[25]: 24, 21, 66 and 9 months for HIV stages I, II, III and IV, respectively. The basic TB model was therefore replicated 5 times, once for HIV uninfected and once for each HIV infected stage, for a total of 42x5 different TB-HIV categories. At each monthly time step (Fig. S1C) HIV uninfected persons became HIV-positive and transitioned to HIV stage I according to the given incidence rate, progressed through the 4 disease stages, and ultimately died and exited the system. Because Currie *et al*.[26] grouped the uninfected and early HIV-infected (stages I and II), the time lag between the HIV and TB declines is longer than in our study, where we allowed for the potential increase in susceptibility to TB infection and progression to occur in earlier HIV stages.[14,27] In the model, HIV induced death mimicked a TB process in that persons in HIV stage IV died of AIDS according to a fixed HIV mortality rate under the competing rates formulation. Accordingly, persons died of either TB or HIV, but not of both (Table S3).

Model Formulation

Under our model formulation all TB processes, and both background and HIV mortality, act as competing rates within a continuous deterministic framework that is updated on discrete monthly time steps. We used a discrete time difference equations formulation, because it is better suited to modeling precise durations of treatment than an exclusively continuous formulation using ordinary differential equations (see Methods, main Article).[8,28,29] This approach provides an approximation to the exact solution of a deterministic model which allowed HIV progression of stages I to IV to occur simultaneously to the progression through the various TB categories, but restricted each individual to undergo one TB state transition (and background and HIV mortality) per time step. That is, at each time step, any given individual could progress in both diseases, in only one, or in neither (Table S3). Below we outline the steps we followed to determine, under this competing rates scheme, the specific rates at which individuals progressed through the different categories of the system when undergoing various multiple processes simultaneously.

Competing rates example. Consider a pool of individuals C, subject to two competing processes: they go to class A at per capita rate α, and to class G at per capita rate γ. The differential equation describing class C is thus:

$$\frac{dC}{dt} = -(\alpha + \gamma) C$$

This simple equation can be solved exactly, yielding:

$$C(t + \Delta t) = C(t) \exp\left[-(\alpha + \gamma)\Delta t\right]$$

If $\Delta t = 1$ timestep, the proportion of individuals remaining in class C at the end of the timestep is $\exp[-(\alpha+\gamma)]$. The proportion of individuals leaving class C is $1-\exp[-(\alpha+\gamma)]$, of whom a fraction $\alpha/(\alpha+\gamma)$ go to class A and $\gamma/(\alpha+\gamma)$ go to class G.

To update the system we use the following convention. We calculate the total leaving rate for each model class, a vector called 'exit_rates'; for the above example the value of exit_rates would be $\alpha+\gamma$. In each time step, beginning with a state vector X_{init}, we calculate the number of individuals that remain in class p as:

$$Z[p] = \exp(-\text{exit\_rates}[p])\, X_{\text{init}}[p].$$

The number leaving class p is $\{1-\exp(-\text{exit\_rates}[p])\}\, X_{\text{init}}[p]$. The individuals that leave each class now distribute themselves into the different TB classes according to the rates determined by each process. For compactness of notation we introduce an intermediate vector Y with elements that are normalized by the total exit rate per state:

$$Y[p] = (1/\text{exit\_rates}[p])\{1-\exp(-\text{exit\_rates}[p])\}\, X_{\text{init}}[p].$$

Now if the per capita transition rate from class p to class q is α_{pq} , the number of individuals making the transition from p to q is simply $\alpha_{pq} Y[p]$. In the above example, $\text{exit\_rates}[C] = \alpha+\gamma$, so $Z[C] = \exp[-(\alpha+\gamma)]\, X_{\text{init}}[C]$ and $Y[C]=\{1/(\alpha+\gamma)\}\{1-\exp[-(\alpha+\gamma)]\}$ $X_{\text{init}}[C]$. The transition rate from class C to class A is α, so the number of individuals making that transition in one time step is $\alpha Y[C]=\{\alpha/(\alpha+\gamma)\}\{1-\exp[-(\alpha+\gamma)]\}X_{\text{init}}[C]$.

Model equations

The state vector X represents the number of individuals in each of the 210 TB-HIV states described in Table S1 and depicted in Fig. S1. Parameters used in the model are

defined in Table S2. The total population is $N = \sum_{i=1}^{42}\sum_{j=1}^{5} X[i,j]$, where i = TB category and j = HIV category.

The force of infection $c_j \lambda$, describing the hazard rate of infection for each susceptible individual (where c_j is the factor corresponding to each HIV stage, Table S2), is calculated from the weighted sum of all infectious classes:

$$\lambda = \frac{1}{N}\sum_{j=1}^{5} \left\{ \beta_{\mathrm{P}}\left(X[4,j]+X[7,j]\right) + \beta_{\mathrm{N}}\left(X[5,j]+X[8,j]\right) + \beta_{\mathrm{PD}}\sum_{m=9}^{16} X[m,j] + \beta_{\mathrm{PN}}\sum_{m=17}^{24} X[m,j] + \ldots \right.$$
$$\left. \beta_{\mathrm{ND}}\sum_{m=26}^{33} X[m,j] + \beta_{\mathrm{NN}}\sum_{m=34}^{41} X[m,j] + \beta_{\mathrm{PF}} X[25,j] + \beta_{\mathrm{NF}} X[42,j] \right\}.$$

We now apply the competing rates formulation described above. The total exit rates for each state are described in Table S3. We label the state vector at the beginning and end of the time steps X_{init} and X_{next}, respectively, and reconcile this from one interval to the next by the relationship:

$$X_{\mathrm{init}}[i,j]_{t+1} = X_{\mathrm{next}}[i,j]_t,$$

where the subscript t refers to the interval under consideration. For simplicity we drop the time t subscript throughout. The number of individuals remaining in each class is then given by the vector Z with elements for HIV categories 1-4:

$$Z[i,j] = \exp(-\text{exit\_rates}[i,j])\, X_{\mathrm{init}}[i,j] \text{ for all } i \text{ and } j=1,\ldots,4.$$

For the final HIV stage IV (category 5) we also needed to account for the additional death rate from AIDS μ_{H} (Table S2). This additional outflow occurred simultaneously to the other TB processes, but because it implies permanent removal from the system it was not reincorporated into the inflows $\xi_{i,j}$ (see below):

$$Z[i,5] = \exp(-\text{exit\_rates}[i,5] - \mu_{\mathrm{H}})\, X_{\mathrm{init}}[i,5] \text{ for all } i.$$

The intermediate vector Y has the following elements for HIV categories 1-4:

$Y[i,j] = (1/\text{exit\_rates}[i,j])\ \{1-\exp(-\text{exit\_rates}[i,j])\}\ X_{\text{init}}[i,j]$, for all i and j=1,…,4,

and for HIV category 5 they are:

$Y[i,5] = (1/\text{exit\_rates}[i,5]+\mu_H)\ \{1-\exp(-\text{exit\_rates}[i,5]-\mu_H)\}\ X_{\text{init}}[i,5]$, for all i.

We then calculated the state vector X_{next}. For clarity purposes, we first describe the equations $\xi_{i,j}$ representing the inflows to each category due to TB infection and treatment (these equations are identical for HIV stages j = 1…5):

$\xi_{i,j}[1,j] = \nu N$

$\xi_{i,j}[2,j] = p_S(\lambda Y[1,j] + b\lambda Y[6,j]) + \pi(Y[4,j] + Y[7,j] + Y[5,j]+Y[8,j])$

$\xi_{i,j}[3,j] = (1-p_S)\ (\lambda Y[1,j] + b\lambda Y[2,j] + b\lambda Y[6,j])$

$\xi_{i,j}[4,j] = s_P(1-d_P)\ (\phi_S Y[2,j] + \phi_F Y[3,j]) + \sigma Y[5,j] + (1-d_P)\rho Y[25,j]$

$\xi_{i,j}[5,j] = (1-s_P)(1-d_N)\ (\phi_S Y[2,j] + \phi_F Y[3,j]) + (1-d_N)\rho Y[42,j]$

$\xi_{i,j}[6,j] =$

$$\sum_{m=1}^{8}\left\{(1-v_D)K_D\left(Z[8+m,j]+Z[25+m,j]\right)+(1-v_N)K_N\left(Z[16+m,j]+Z[33+m,j]\right)\right\}$$

$\xi_{i,j}[7,j] = s_P\, d_P\ (\phi_S Y[2,j] + \phi_F Y[3,j]) + \sigma Y[8,j] + d_P\rho Y[25,j]$

$\xi_{i,j}[8,j] = (1-s_P)\, d_N(\phi_S Y[2,j] + \phi_F Y[3,j]) + d_N\rho Y[42,j]$

$\xi_{i,j}[9,j] = \theta t_P Y(7,j)$

$\xi_{i,j}[9+m,j] = Z[9+m-1,j]\ (1-K_D[m]), \quad m = 1,2,\ldots,7$

$\xi_{i,j}[17,j] = \theta(1-t_P)Y(7,j)$

$\xi_{i,j}[17+m,j] = Z[17+m-1,j]\ (1-K_N[m]),\ m = 1,2,\ldots,7$

$\xi_{i,j}[25,j] =$

$$\sum_{m=1}^{8} \left\{\delta_{\mathrm{D}} Y[8+m,j] + \delta_{\mathrm{N}} Y[16+m,j] + v_{\mathrm{D}} K_{\mathrm{D}}[m] Z[8+m,j] + v_{\mathrm{N}} K_{\mathrm{N}}[m] Z[16+m,j]\right\}$$

$\xi_{i,j}[26,j] = \theta t_{\mathrm{N}} Y(8,j)$

$\xi_{i,j}[26+m,j] = Z[26+m-1,j]\ (1-K_{\mathrm{D}}[m]),\ m = 1,2,\ldots,7$

$\xi_{i,j}[34,j] = \theta(1-t_{\mathrm{N}}) Y(8,j)$

$\xi_{i,j}[34+m,j] = Z[34+m-1,j]\ (1-K_{\mathrm{N}}[m]),\ m = 1,2,\ldots,7$

$\xi_{i,j}[42,j] =$

$$\sum_{m=1}^{8} \left\{\delta_{\mathrm{D}} Y[25+m,j] + \delta_{\mathrm{N}} Y[33+m,j] + v_{\mathrm{D}} K_{\mathrm{D}}[m] Z[25+m,j] + v_{\mathrm{N}} K_{\mathrm{N}}[m] Z[33+m,j]\right\}$$

To account for the simultaneous occurrence of HIV infection and progression, we introduced the parameter Ψ_j (Table S2). The first element of Ψ_j reflected HIV incidence values that generated reported HIV prevalence levels[24], the next 3 elements represented progression of HIV stages I-III[25], and the fifth element had a value of 0, since there is no transition beyond stage IV (only death, which was accounted for separately as a competing rate to TB process transitions, see above and Table S3). At each time step the new X_{next} was calculated by the sum of the persons staying in the corresponding TB and HIV category, those progressing in only one disease, and those progressing in both. Accordingly, the HIV-uninfected category is updated with those persons that remain HIV uninfected (1- Ψ_1) and either do not progress in their TB category ($Z[i,1]$) or do ($\sum_{i=1}^{42} \xi_{i,1}$):

$$X_{\mathrm{next}}[i,1] = (1-\Psi_1)\ (Z[i,1] + \sum_{i=1}^{42} \xi_{i,1}) \qquad \text{for } i = 1\text{-}42.$$

Likewise, the HIV infected categories are updated with persons that remain in that same HIV category (1- Ψ_j) and either do not progress in their TB category ($Z[i,j]$) or do ($\sum_{i=1}^{42}\sum_{j=2}^{5}\xi_{i,j}$). The difference with the HIV uninfected category (j = 1 above) lies in that now we also have to account for those persons that either became infected or progressed from the previous HIV stage (Ψ_{j-1}), together with their TB dynamics, i.e., include those persons that did not progress in their TB category ($Z[i,j-1]$), or that did ($\sum_{i=1}^{42}\sum_{j=2}^{5}\xi_{i,j-1}$):

$$X_{\text{next}}[i,j] = (1-\Psi_j)\,(Z[i,j]+\sum_{i=1}^{42}\sum_{j=2}^{5}\xi_{i,j}) + \Psi_{j-1}\,(Z[i,j-1]+\sum_{i=1}^{42}\sum_{j=2}^{5}\xi_{i,j-1})$$

for i = 1-42, and j = 2-5.

At any given time point, the number of persons in each HIV disease stage was determined by the year since the HIV epidemic began, by the average time spent in each HIV disease stage, and by the HIV prevalence. People become infected (i.e., move from the HIV uninfected stage into the HIV infected stage I, a process which corresponds to HIV incidence Ψ_1), progress through the subsequent HIV stages II-IV (Ψ_2– Ψ_4) and ultimately die of HIV (μ_H) according to the time frames given by Morgan *et al.*[25] for Africa. Our model formulation allows us to emulate the historical estimates of HIV prevalence (i.e., the sum of all the persons in HIV stages I through IV) as reported for Kenya[24] by altering the HIV incidence (Fig. S2).

In the equations referring to treatment states in the model, we include the "switch" variables K_D and K_N, which are vectors containing the monthly probabilities that a course of treatment ends. For conventional drug therapies, these are:

K_D=[0 0 0 0 0 0 1 0 0] for six-month DOTS treatment, and

K_N=[0 0 0 0 0 0 0 1] for eight-month non-DOTS treatment.

New TB cases were computed as the sum of the flows from the latently infected, both slow and fast, and of the progressors from the failed treatment class, both smear-positive and smear-negative:

$$New\_TBcases = \sum_{j=1}^{5} \left(\phi_S Y_{2j} + \phi_F Y_{3j} + \rho_P Y_{25j} + \rho_N Y_{42j} \right).$$

Model Calibration

The conventional measure for goodness-of-fit, GF = (Obs - Exp)^2/Exp, places greater weight on instances where observed values exceed expected values (Obs > Exp) than those where Obs < Exp. We used a related measure that is symmetric with respect to Obs versus Exp (see Methods, main Article) at the expense of losing the statistical convenience of the chi-squared distributional properties of the conventional measure, because the observed values are not necessarily more reliable than the expected when the former incorporate numerous uncertainties related to disease surveillance while the latter integrate numerous sources of knowledge via a mathematical model.

Working in a gradual process with our candidate parameter sets, we evaluated the fit of the model outcome for each set to the TB and TB-HIV Kenyan measures spanning 1980 to 2004 by a feedback calibration process. Each parameter set was run as a separate simulation that started in the initial virgin phase, and progressed through the subsequent three phases characterizing the TB epidemic in Kenya during the last century and early part of the 21st century (i.e., until 2006). If any parameter values in the best goodness-of-fit (see Methods and below) set were at the margin of the pre-defined ranges, we shifted the range by 5% or 10%, depending on the breadth of the original range. Additionally, we

restricted the original range if the 20 best *GF* parameter sets were in a close neighbourhood. We generated additional parameters sets with the LHS method, whose values fell within the constraints of the new parameter ranges, and ran further simulations. This approach permitted us to modify our designation of the parameter ranges characterizing the person-level processes according to the fit of the model to the 25-year country-level data. This iterative procedure involved >30,000 simulations. For the calibration with the final ranges, we ran >6,000 parameter sets. In our subsequent calibration conducted to match the model output to the full 1980-2004 TB and TB-HIV dataset, we used the same final parameter sets (and therefore the same parameter ranges and constraints) derived from our earlier fit to the reported HIV trends.[24] However, in this last calibration we modified the HIV incidence such that HIV prevalence increased monotonically at different rates to a final 2004 value that ranged between 10%-25%, resulting in >37,000 runs.

When comparing the results obtained for the best-fitting parameter sets to the TB and TB-HIV measures up to 1997 as compared to the full data set (Table S2), we observed: (*i*) susceptibility to becoming TB infected was higher in stage II, although smaller for the other 3 infection force values across HIV stages (λ_j), and interestingly this parameter had a greater impact on TB incidence changes in the full dataset vs. the pre-1997 dataset (Table 1), (*ii*) patients transiently recovered were more infectious (β_{TR} = 0.54 vs. 0.26) and (*iii*) default rates were higher (*bD* = 0.027 vs. 0.02). Otherwise the parameter estimates for the two calibrations were very similar for HIV uninfected and HIV stages I and II. Values were less similar for parameters characterizing HIV stage IV. This is partly

due to these being parameters of lesser impact (Table 1), which is compounded by the inherent limitations of the calibration to country-level data.

We were also interested in understanding how the country-level calibration to the pre-1997 and the full datasets resolved the relative values of the parameters characterizing TB processes in HIV infected persons in stages I and II. With this process in essence we are deriving individual-level, clinical parameters for the different HIV stages from population-level data. It is interesting to note that although the relative magnitudes of the pertinent 8 parameter types across HIV stages I and II were not constrained in the calibration (λ_j, $p_{S,j}$, π_j, ρ_j, $s_{P,j}$, σ_j, θ_j, $q_{c,j}$, where $j = 0$ indicates HIV uninfected, and $j = 1$-4 indicates HIV stage I-IV, respectively, see Table S2 for ranges), when we calibrated the model to the pre-1997 dataset all parameters ordered themselves in the expected increasing or decreasing order according to HIV stage. When we used the full dataset only two parameters had their values inverted with respect to those expected under a progressive immune deterioration from the moment of HIV infection. Most importantly, the case-detection rates θ_1 and θ_2 had inverted values: $\theta_1 = 0.18 > \theta_2 = 0.16$ (in any case the ranges for θ_1 and θ_2 completely overlapped, while those of the other parameters did not, see Table S2). When we exchanged the values for θ_1 and θ_2, the *GF* became worse. Therefore, under this calibration the strikingly non-matching HIV and TB trends are best tracked by assuming that more TB infections are detected in persons in HIV stage I than in HIV stage II.

In addition, the rates for spontaneous recovery to latency in HIV stages I and II, Δ_1 and Δ_2, were also inverted in relative magnitude as compared to those expected under the general HIV progression scenario (0.119 and 0.112, respectively). We believe this

ordering reflects the fact that we cannot work with an infinite sample of parameter sets covering all the possible parameter combinations—due to computational limitations we have to settle for a limited sample of combinations, obtained in our case with the LHS method from all the possible combinations of the parameter space—rather than actual epidemiological interpretations of the calibration process to the reported disease trends. There are two reasons for this argument: a) these two values have very similar magnitudes, b) according to the sensitivity analysis these parameters do not have a great impact on TB incidence, so that small differences between them are not expected to have a large impact on the epidemic's course and therefore on their predictive value (Fig. 4 and Table S4), and c) the *GF* score decreased when we exchanged the values.

Under the calibration to reported HIV trends, our model predicts that in 2004 the proportion of HIV infected persons among the TB infected is 43%. This value is closer to the 50% value reported for countries of high HIV prevalence in the general population[30] than to the 29% estimate for Kenya.[2] Moreover, recent surveillance efforts in Kenya indicate that past surveys may have seriously underestimated the proportion of HIV infected among TB cases. In essence, even though under our calibration to the declining HIV epidemic the model is not matching up to the reported increase in TB case notifications (Fig. 1), it still needs to account for the resulting lower-than-reported TB trends by having a greater-than-reported proportion of TB-HIV coinfected people.

In our calibration to the monotonically increasing HIV epidemic we focused on matching the TB case notifications. Accordingly, the fit to the TB case notifications improved substantially (0.42 vs. 0.08), while the overall fit to the full dataset worsened (from 6.2 to 7.4) in comparison to that of the best-fit parameter set under the calibration

to reported HIV trends. The measures most responsible for the increase in the GF involved TB measures in HIV infected persons in the most recent years, particularly TB deaths in HIV infected and the proportion of TB cases that are HIV infected. When these two measures are not included in the calculation of the GF, then the overall fit to the full dataset under the monotonically increasing HIV epidemic is better than that under the reported HIV trends (4.9 vs. 5.5). Most significantly, the fit to the TB incidence in later years, and the fit to TB mortality in both early and later years, improved under the calibration to the monotonically increasing HIV epidemic.

Assumptions and limitations of the study

As with practically any mathematical analysis of a biological system, our model formulation cannot capture its full complexity, and the overall modeling exercise entails various limitations. We cannot exclude the possibility that the mismatch between reported trends and model output arises because the model does not accurately reflect the epidemiological mechanisms at play. In this light, however, it is important to note that another model of TB-HIV co-dynamics (with a different structure from the model reported here) is also incapable of reconciling declining HIV prevalence with increasing TB incidence (Currie, pers. comm.). To further address these concerns, we extended our investigation to consider TB-HIV trends across Africa (see main Article). We were however careful to design a model that reflected the key processes that would permit us to enhance our understanding of TB-HIV co-epidemiology, particularly in regards to our original question (see main Article). An additional limitation to studies of this nature is the great uncertainty in the parameter values, which requires us to conduct a calibration

in order to identify the optimum parameter set for portraying TB-HIV trends in a particular setting (i.e., Kenya in our case). This uncertainty is not only due to our limited knowledge of the system, but also to the considerable heterogeneity regarding TB and HIV trends between and within countries, both in space and time (see main Article). Even though the calibration enables us to track reported epidemiological trends more precisely, it is also laden with assumptions because for many parameters we do not have a proper understanding of the minimum and maximum numerical values they can have (i.e., their valid ranges, see above). Moreover, there could be compensatory effects among the parameters that could lead us to choose a parameter set that does not correspond to the actual values characterizing the process in the field, but that tracks the reported trends (themselves questionable, see below) with high fidelity. Because of the important limitations regarding our biological understanding of the system, the most appropriate way to modify the model to provide a better fit to reported TB-HIV trends comes from increasing our knowledge on TB-HIV interactions and public health control and surveillance, and not intrinsically from an analysis of the model.

When interpreting the results of the sensitivity analysis (see main Article) we must keep in mind that it offers information not only on the biological processes and public health control measures with the greatest potential to impact our measure of choice (e.g., TB incidence), but also on how our uncertainty in the parameter estimates impacts the uncertainty in the model outcome.[26,31,32] Consequently, given our large degree of uncertainty regarding both the most suitable parameter ranges characterizing TB-HIV processes, and the reliability of nationwide epidemiological trends, our results should be interpreted with caution. Moreover, as with any sampling method, the sampling strategy

for the parameters will impact the distribution of outcomes (see above). As we refine our knowledge on TB and HIV interactions we will limit our sources of uncertainty regarding the co-dynamics of the two pathogens. Accordingly, the parameter ranges should then reflect to a lesser degree our lack of understanding of the system, and more the actual temporal and spatial variation characterizing TB-HIV co-dynamics. More precise knowledge on parameter values will enable more robust policy recommendations to be derived from sensitivity analyses of epidemic models.

References

1. World Health Organization. WHO Global TB Database. Available from: http://www.who.int/tb/country/global_tb_database/en/index.html; 2006.
2. World Health Organization. *Global Tuberculosis Control: Surveillance, Planning, Financing: WHO report 2006*. Geneva: World Health Organization; 2006.
3. World Health Organization.*Global Tuberculosis Control. WHO Report 2001.* Geneva: World Health Organization; 2001.
4. World Health Organization. *Global Tuberculosis Control. Surveillance, planning, financing. WHO report 2002.* Geneva: World Health Organization; 2002.
5. World Health Organization. *Global Tuberculosis Control. Surveillance, planning, financing. WHO report 2003.* Geneva: World Health Organization; 2003.
6. World Health Organization. *Global Tuberculosis Control:surveillance, planning, financing. WHO report 2004.* Geneva: World Health Organization; 2004.

7. World Health Organization. *Global Tuberculosis Control:surveillance, planning, financing. WHO report 2005.* Geneva: World Health Organization; 2005.

8. Salomon JA, Lloyd-Smith JO, Getz WM, Resch S, Sánchez MS, Porco TC, et al. Prospects for advancing tuberculosis control efforts through novel therapies. *PLoS Med* 2006;3:e273.

9. Reichman LB, Hershfield ES. *Tuberculosis. A comprehensive international approach.* New York: Marcel Dekker, Inc., 2000.

10. Frieden TR, Sterling TR, Munsiff SS, Watt CJ, Dye C. Tuberculosis. *Lancet* 2003;362:887-99.

11. Maher D, Harries A, Getahun H. Tuberculosis and HIV interaction in sub-Saharan Africa: impact on patients and programmes; implications for policies. *Trop Med Int Health* 2005;10:734-42.

12. Keshinro B, Diul MY. HIV-TB: epidemiology, clinical features and diagnosis of smear-negative TB. *Trop Doct* 2006;36:68-71.

13. Sonnenberg P, Murray J, Glynn JR, Shearer S, Kambashi B, Godfrey-Faussett P. HIV-1 and recurrence, relapse, and reinfection of tuberculosis after cure: a cohort study in South African mineworkers. *Lancet* 2001;358:1687-93.

14. Fox J, Weber J, Fidler S. Primary HIV. *Sex Transm Infect* 2006;82:267-8.

15. Corbett EL, Charalambous S, Moloi VM, Fielding K, Grant AD, Dye C, et al. Human Immunodeficiency Virus and the Prevalence of Undiagnosed Tuberculosis in African Gold Miners. *Am J Respir Crit Care Med* 2004;

16. Chakaya JM, Meme H, Kwamanga D, Githui WA, Onyango-Ouma WO, Gicheha C, et al. Planning for PPM-DOTS implementation in urban slums in Kenya:

knowledge, attitude and practices of private health care providers in Kibera slum, Nairobi. *Int J Tuberc Lung Dis* 2005;9:403-8.

17. Noor AM, Amin AA, Gething PW, Atkinson PM, Hay SI, Snow RW. Modelling distances travelled to government health services in Kenya. *Trop Med Int Health* 2006;11:188-96.

18. Dowdy DW, Chaisson RE, Moulton LH, Dorman SE. The potential impact of enhanced diagnostic techniques for tuberculosis driven by HIV: a mathematical model. *AIDS* 2006;20:751-62.

19. Mtei L, Matee M, Herfort O, Bakari M, Horsburgh CR, Waddell R, et al. High rates of clinical and subclinical tuberculosis among HIV-infected ambulatory subjects in Tanzania. *Clin Infect Dis* 2005;40:1500-7.

20. Hopewell PC, Pai M. Tuberculosis, vulnerability, and access to quality care. *JAMA-J Am Med Assn* 2005;293:2790-3.

21. Day JH, Grant AD, Fielding KL, Morris L, Moloi V, Charalambous S, et al. Does tuberculosis increase HIV load? *J Infect Dis* 2004;190:1677-84.

22. Kannangara S, DeSimone JA, Pomerantz RJ. Attenuation of HIV-1 infection by other microbial agents. *J Infect Dis* 2005;192:1003-9.

23. Lawn SD. AIDS in Africa: the impact of coinfections on the pathogenesis of HIV-1 infection. *J Infect* 2004;48:1-12.

24. Cheluget B, Baltazar G, Orege P, Ibrahim M, Marum LH, Stover J. Evidence for population level declines in adult HIV prevalence in Kenya. *Sex Transm Infect* 2006;82:I21-I6.

25. Morgan D, Mahe C, Mayanja B, Okongo JM, Lubega R, Whitworth JAG. HIV-1 infection in rural Africa: is there a difference in median time to AIDS and survival compared with that in industrialized countries? *AIDS* 2002;16:597-603.

26. Currie CS, Williams BG, Cheng RC, Dye C. Tuberculosis epidemics driven by HIV: is prevention better than cure? *AIDS* 2003;17:2501-8.

27. Sonnenberg P, Glynn JR, Fielding K, Murray J, Godfrey-Faussett P, Shearer S. How soon after infection with HIV does the risk of tuberculosis start to increase? A retrospective cohort study in South African gold miners. *J Infect Dis* 2005;191:150-8.

28. Getz WM, Lloyd-Smith JO. Basic methods for modeling the invasion and spread of contagious diseases. In: *Disease Evolution: Models, Concepts and Data Analyses.* Edited by Fenge Z, Dieckmann U, Levin SA: AMS-DIMACS Series; 2006.

29. Getz WM, Lloyd-Smith JO, Cross PC, Bar-David S, Johnson PL, Porco TC, et al. Modeling the Invasion and Spread of Contagious Diseases in Heterogeneous Populations. In: *Disease Evolution: Models, Concepts and Data Analyses.* Edited by Fenge Z, Dieckmann U, Levin SA: AMS-DIMACS Series; 2006.

30. Dye C. Global epidemiology of tuberculosis. *Lancet* 2006;367:938-40.

31. Blower SM, Dowlatabadi H. Sensitivity and Uncertainty Analysis of Complex-Models of Disease Transmission - an HIV Model, as an Example. *Intern Stat Rev* 1994;62:229-43.

32. Saltelli A, Chan K, Scott EM. *Sensitivity Analysis*. West Sussex, England: Wiley, 2000.

33. CIA. **World Factbook**. Available from: https://www.cia.gov/cia/publications/factbook/geos/ke.html; 2003.

34. Jaffar S, Grant AD, Whitworth J, Smith PG, Whittle H. The natural history of HIV-1 and HIV-2 infections in adults in Africa: a literature review. *Bull World Health Organ* 2004;82:462-9.

35. Dye C, Williams BG. Criteria for the control of drug-resistant tuberculosis. *Proc Natl Acad Sci USA* 2000;97:8180-5.

36. Dye C, Garnett GP, Sleeman K, Williams BG. Prospects for worldwide tuberculosis control under the WHO DOTS strategy. Directly observed short-course therapy. *Lancet* 1998;352:1886-91.

37. Murray CJ, Salomon JA. Modeling the impact of global tuberculosis control strategies. *Proc Natl Acad Sci USA* 1998;95:13881-6.

Table S1. State variables for TB and HIV.

TB State (*i*)	Abbrev.	Definition
1	S	TB susceptible
2	IS	TB infection, slow progressor (latent)
3	IF	TB infection, fast progressor
4	AP	Smear-positive active TB, not detectable
5	AN	Smear-negative active TB, not detectable
6	R	TB recovered
7	APd	Smear-positive active TB, detectable
8	ANd	Smear-negative active TB, detectable
9-16	TPD	Smear-positive TB case undergoing DOTS treatment, months 1-8
17-24	TPN	Smear-positive TB case undergoing non-DOTS treatment, months 1-8
25	TPF	TB treatment failure, smear-positive case
26-33	TND	Smear-negative TB case undergoing DOTS treatment, months 1-8

34-41	TNN	Smear-negative TB case undergoing non-DOTS treatment, months 1-8
42	TNF	TB treatment failure, smear-negative case

HIV State (*j*)	**Abbrev.**	**Definition**
1	U	HIV uninfected
2	I	HIV infected stage I
3	II	HIV infected stage II
4	III	HIV infected stage III
5	IV	HIV infected stage IV

The distribution of the population across different TB states is presented as a 42-element vector, while that of HIV as a 5-element vector, for a total of 42x5 combined TB-HIV categories.

Table S2. Model parameters.

	Definition and units when applicable♠	HIV– (j = 1)	HIV+ stage I (j = 2)	HIV+ stage II (j = 3)	HIV+ stage III (j = 4)	HIV+ stage IV (j = 5)	Source
Population parameters							
ν	total population growth (persons per 1000 individuals per year)	64 (computed to achieve reported population growth rate)					NA
μ	natural mortality rate per year	0.016					[33]
HIV parameters							
$\Psi_{j,}$	HIV incidence Ψ_1 (rate at which persons become newly infected with HIV) progression Ψ_{2-4} (rate of progression to next HIV stage)	calibration to trends in [24]	0.0417	0.0476	0.0152	0*	[25,34]
μ_H	HIV mortality rate per year	NA	NA	NA	NA	0.1111	[25,34]

TB infection parameters

$c_j\lambda$	force of infection – computed** (rate at which persons become newly infected with TB)	1λ	1.26λ {1.19λ} (1λ –1.4λ)	1.34λ {1.4λ} (1.2λ – 1.6λ)	1.67λ {1.62λ} (1.6λ – 2.3λ)	4.21λ {3.72λ} (2.5λ –5λ)	calibration
β_P	number of new infections per untreated SS+ case			0.78 {0.79} (0.7-1.05)			[a]
β_N	number of new infections per untreated SS– case			$0.15\beta_P$			[b]
β_{PD} β_{ND} β_{PN} β_{NN} β_{NF}	number of new infections per treated case and per SS– case that has failed treatment			0			[8]
β_{PF}	number of new infections per SS+ case that failed treatment			0.26 {0.54} (0.15-0.92)			[8], [a] and calibration
b	relative susceptibility to reinfection for latent slow progressors and recovered	0.35	0.5	0.6	0.7	0.8	[a]

TB natural history parameters

p_S	proportion of new TB infections entering latent slow-progressor pool	0.82 {0.84} (0.8-0.95)	0.59 {0.6} (0.55-0.85)	0.58 {0.57} (0.45-0.75)	0.43 {0.36} (0.25-0.45)	0.28 {0.05} (0.0-0.3)	[a] and calibration
ϕ_S	breakdown rate for slow progressors (endogenous reactivation)	.00013/12	0.0002/12	0.001/12	.06/12	.1/12	[26] and [a]
ϕ_F	breakdown rate for fast progressors	0.88/12	0.9/12	1/12	2/12	4/12	[a] and calibration
s_P	proportion of new active cases with SS+ disease	0.51 {0.52} (0.45-0.57)	0.48 {0.48} (0.425-0.525)	0.48 {0.48} (0.40-0.50)	0.40 {0.42} (0.20-0.45)	0.20 {0.11} (0.0-0.20)	[a], [b] and calibration
d	proportion of new cases entering detectable pool						calibration
	a) preDOTS, no HIV (1960-1979)			0-0.5			
	b) preDOTS, HIV (1980-1994)			0.5-0.6			
	c) DOTS, HIV (1995-2004)			0.6-0.8			

σ	rate of conversion from SS− to SS+ disease	0.0019 {0.0019} (0.0016-0.0021)	0.0014 {0.0015} (0.0013-0.0018)	0.0012 {0.0015} (0.0011-0.0016)	0.001 {0.0009} (0.0007-0.0011)	0.0004 {0.0005} (0.0-0.0007)	calibration
π	rate of spontaneous recovery to latency	0.032 {0.032} (0.017-0.033)	0.017 {0.015} (0.012-0.020)	0.008 {0.012} (0.007-0.016)	0.005 {0.006} (0.0025-0.0065)	0.001 {0.0001} (0.0-0.0011)	[a] and calibration
μ_P	TB mortality rate, untreated SS+	0.3/12	0.3/12	0.32/12	0.8/12	1/12	[a] and [26]
μ_N	TB mortality rate, untreated SS−	0.2/12	0.2/12	0.21/12	0.8/12	1/12	calibration

TB treatment parameters

θ	case-detection rate	0.12 {0.09} (0.08-0.15)	0.14 {0.18} (0.10-0.20)	0.17 {0.16} (0.10-0.20)	0.3 {0.25} (0.20-0.40)	0.75 {0.45} (0.40-0.80)	calibration
t_P	proportion of SS+ treated cases entering DOTS programs						[2]
	a) preDOTS, no HIV			0			
	b) preDOTS, HIV			0			
	c) DOTS, HIV			0-0.56			

t_N	proportion of SS- treated cases entering DOTS programs		[2]
	a) preDOTS, no HIV	0	
	b) preDOTS, HIV	0	
	c) DOTS, HIV	0-0.71	
δ_6	default rate for 6- and 8-month programs, month m	δ_6 = monthlyFactor*baseDefault, where	[8] and calibration
	monthlyFactor***	m (1) = 1	
		m (2) = 3	
		m (3) = 2	
		m (4-8) = 1	
	baseDefault	D = 0.02 {0.027} (0.01-0.03)	

q_{PD} q_{PN} [m=1:8] proportion of SS+ cases defaulting from month m of treatment that return to active disease [2,8] and calibration

m = 1	0.8	0.8	0.85	0.95	1
m = 2	0.5	0.6	0.75	0.9	1
m = 3	0.3	0.5	0.7	0.875	1
m = 4	0.2	0.4	0.65	0.85	1
m = 5	0.1	0.35	0.6	0.825	1
m = 6	0.01	0.3	0.5	0.8	1
m = 7	0.01	0.3	0.5	0.8	1
m = 8	0.01	0.3	0.5	0.8	1

q_{ND} q_{NN} [m=1:8]	proportion of SS- cases defaulting from month m of treatment that return to active disease	$q_{N1} = 0.9q_{P1}$	$q_{N2} = 0.9q_{P2}$	$q_{N3} = 0.9q_{P3}$	$q_{N4} = 0.9q_{P4}$	$q_{N5} = 0.9q_{P5}$	[2,8] and calibration
v_{kl} [m=1:8]	proportion of SS+ and SS- cases defaulting from month m of treatment that enter failed treatment class	$v_{kl} = 1 - q_{kl}$, where k = P represents SS+ k = N represents SS- l = D represents DOTS l = N represents non-DOTS					[2,8] and calibration
$q_{complete}$	proportion of cases that return to active disease after completing treatment	0.12 {0.14} (0.05-0.15)	0.18 {0.19} (0.10-0.20)	0.21 {0.25} (0.15-0.25)	0.26 {0.31} (0.25-0.35)	0.43 {0.35} (0.35-0.50)	[2,8] and calibration
$v_{complete}$	proportion of cases that enter failed treatment class after completing treatment	0.14 {0.13} (0.05-0.20)	0.10 {0.21} (0.10-0.23)	0.21 {0.17} (0.15-0.25)	0.33 {0.33} (0.20-0.35)	0.34 {0.32} (0.30-0.50)	[2,8] and calibration
$s_{complete}$	proportion of cases cured after completing treatment	$s_{complete} = 1 - v_{complete} - q_{complete}$					
ρ	relapse rate from failed treatment class to active disease	0.088 {0.083} (0.06-0.10)	0.118 {0.119} (0.097-0.127)	0.126 {0.112} (0.105-0.135)	0.172 {0.141} (0.135-0.175)	0.176 {0.222} (0.175-0.325)	[8] and calibration

μ_{PD}	TB mortality, SS+ cases on DOTS treatment						
	$m = 1$	0.320/12	0.320/12	0.424/12	0.536/12	0.800/12	calibration
	$m = 2$	0.160/12	0.160/12	0.216/12	0.264/12	0.480/12	
	$m = 3\text{-}8$	0.040/12	0.040/12	0.040/12	0.048/12	0.056/12	
μ_{ND}	TB mortality, SS- cases on DOTS treatment						calibration
	$m = 1$	0.160/12	0.160/12	0.320/12	0.480/12	0.800/12	
	$m = 2$	0.080/12	0.080/12	0.160/12	0.240/12	0.480/12	
	$m = 3\text{-}8$	0.040/12	0.040/12	0.040/12	0.048/12	0.056/12	
μ_{PN}	TB mortality, SS+ cases on non-DOTS treatment			$\mu_{PN} = 3\mu_{PD}$			calibration
μ_{NN}	TB mortality, SS– cases on non-DOTS treatment			$\mu_{NN} = 3\mu_{ND}$			calibration

Throughout this study we used: a) parameters of fixed value, b) the best-fit parameter values in the pre-1997 calibration, c) the best-fit parameter values in the full dataset calibration in brackets {}, and d) the ranges for those parameters whose values were allowed to vary in the calibrations in parenthesis (). Greek symbols represent rates, lower case Roman symbols represent proportions. Vectors indices are shown in square brackets []. All rates are monthly unless specified otherwise. Constraints for the calibration ranges are

given below. Abbreviations used are NA: not applicable, SS-: smear-negative TB, SS+: smear-positive TB, HIV-: HIV uninfected, HIV+: HIV infected.

♠ for parameters representing rates or proportions, we multiply the parameter value by the total number of persons in the category from which the corresponding process is exiting, in order to obtain the total number of persons at each time step that exits that category due to that particular process

* a value of 0 was given to nullify the impact of the last element of this vector, because persons die from AIDS and exit the system once they reach HIV stage IV, see Model Formulation

** λ = the force of infection, was computed at each monthly time step, see Model Formulation

*** m = month of treatment, which ranges from 8 months for non-DOTS programs and 6 months for present-day DOTS programs

[a] parameter values and ranges adapted from Dye and Williams, 2000[35] and Dye *et al.*, 1998 [36]

[b] parameter values and ranges adapted from Murray and Salomon, 1998[37]

Calibration constraints in relation to HIV stages:

- HIV stage I, HIV stage II < HIV stage III < HIV stage IV for $c_j \lambda$
- HIV uninfected > HIV stage I, HIV stage II > HIV stage III > HIV stage IV for parameters p_S, π, ρ, θ, q_{complete}, s_{complete}

- HIV uninfected < HIV stage I, HIV stage II < HIV stage III < HIV stage IV for parameters for s_P, σ
- $\beta_{TR} < \beta_P$

These constraints were applied to all the pertinent parameters allowed to vary in the calibration, except for $v_{complete}$ (see above) which was unconstrained given that its value is calculated from $s_{complete} + v_{complete} + q_{complete} = 1$, and both $s_{complete}$ and $q_{complete}$ (see above) were constrained as described here. In our analysis we only used those parameter sets generated by the Latin Hypercube Sampling that conformed to these constraints.

Table S3. Exit rates from TB and HIV states in the model.

TB State	TB exit rates	HIV State	HIV exit rates
1	$\lambda + \mu$	1	Ψ_1
2	$\lambda b(1\text{-}p_S) + \phi_S + \mu$	2	Ψ_2
3	$\phi_F + \mu$	3	Ψ_3
4	$\pi + \mu_P + \mu$	4	Ψ_4
5	$\pi + \sigma + \mu_N + \mu$	5	μ_H ($\Psi_5 = 0$)
6	$\lambda b + \mu$		
7	$\theta + \pi + \mu_P + \mu$		
8	$\theta + \pi + \sigma + \mu_N + \mu$		
9-16	$\delta + \mu_{PD} + \mu$		
17-24	$\delta + \mu_{PN} + \mu$		
25	$\rho + \mu$		
26-33	$\delta + \mu_{ND} + \mu$		
34-41	$\delta + \mu_{NN} + \mu$		
42	$\rho + \mu$		

Table S4. Sensitivity analysis results in terms of partial rank correlation coefficients (PRCC).

		PRCC	
		(a) 1997	(b) 2004
force of infection			
1	λ_1	0.179	0.207 (18)
2	λ_2	0.128	0.163
3	λ_3	0.533 (9)	0.531 (9)
4	λ_4	0.025	0.032
number of new infections per untreated SS+ case			
5	β_P	0.848 (1)	0.830 (3)
number of new infections per SS+ case that failed treatment			
6	B_{PF}	0.802 (4)	0.805 (4)
proportion of new TB infections entering latent slow-progressor pool			
7	p_{S0}	-0.711 (7)	-0.697 (7)
8	p_{S1}	-0.374 (11)	-0.341 (13)
9	p_{S2}	-0.272 (16)	-0.318 (15)
10	p_{S3}	-0.327 (15)	-0.310 (16)
11	p_{S4}	0.018	0.009
rate of spontaneous recovery to latency			
12	π_0	-0.143	-0.039
13	π_1	-0.042	-0.026
14	π_2	-0.017	-0.0003
15	π_3	-0.139	-0.125
16	π_4	-0.020	-0.067
relapse rate from failed treatment class to active disease			
17	ρ_0	-0.330 (14)	-0.323 (14)
18	ρ_1	-0.044	-0.073
19	ρ_2	-0.011	0.021
20	ρ_3	-0.041	-0.041
21	ρ_4	-0.032	-0.029
proportion of new active cases with SS+ disease			
22	s_{P0}	0.565 (8)	0.545 (8)
23	s_{P1}	0.035	0.031
24	s_{P2}	0.072	0.137
25	s_{P3}	0.845 (2)	0.844 (1)
26	s_{P4}	0.180	0.177
rate of conversion from SS− to SS+ disease			
27	σ_0	0.007	-0.014
28	σ_1	0.040	0.032
29	σ_2	-0.009	0.001
30	σ_3	0.047	0.012
31	σ_4	-0.016	0.005

base default rate for DOTS and non-DOTS programs			
32	D	0.741 (5)	0.754 (5)
case-detection rate			
33	θ_0	-0.833 (3)	-0.833 (2)
34	θ_1	-0.109	-0.145
35	θ_2	-0.024	-0.070
36	θ_3	-0.405 (10)	-0.443 (10)
37	θ_4	-0.027	0.005
proportion of cases that return to active disease after completing treatment			
38	$q_{\text{complete},0}$	0.356 (13)	0.394 (11)
39	$q_{\text{complete},1}$	0.003	0.050
40	$q_{\text{complete},2}$	0.0004	-0.015
41	$q_{\text{complete},3}$	0.224 (17)	0.219 (17)
42	$q_{\text{complete},4}$	0.004	-0.031
proportion of cases that enter failed treatment class after completing treatment			
43	$v_{\text{complete},0}$	0.715 (6)	0.731 (6)
44	$v_{\text{complete},1}$	0.040	0.110
45	$v_{\text{complete},2}$	0.069	0.043
46	$v_{\text{complete},3}$	0.374 (12)	0.353 (12)
47	$v_{\text{complete},4}$	0.015	0.003

Note: PRCC values for key variables with respect to reductions in incidence when we projected the runs to 2030, relative to 2005, at a stable HIV prevalence of 6.7%. We used the 1,000 parameter sets that provided the best goodness-of-fit (*GF*) scores (Fig. 1) when the model was calibrated to fit TB and HIV data in Kenya up to, and including: (a) 1997, and (b) 2004. Numerical subindices indicate HIV infection status (0, uninfected, and numbers 1-4 correspond to the WHO HIV disease stages I-IV). We include the relative ranking of the PRCCs in parenthesis, with only those with absolute values >0.2 ranked.

Fig. S1. Study schematic.

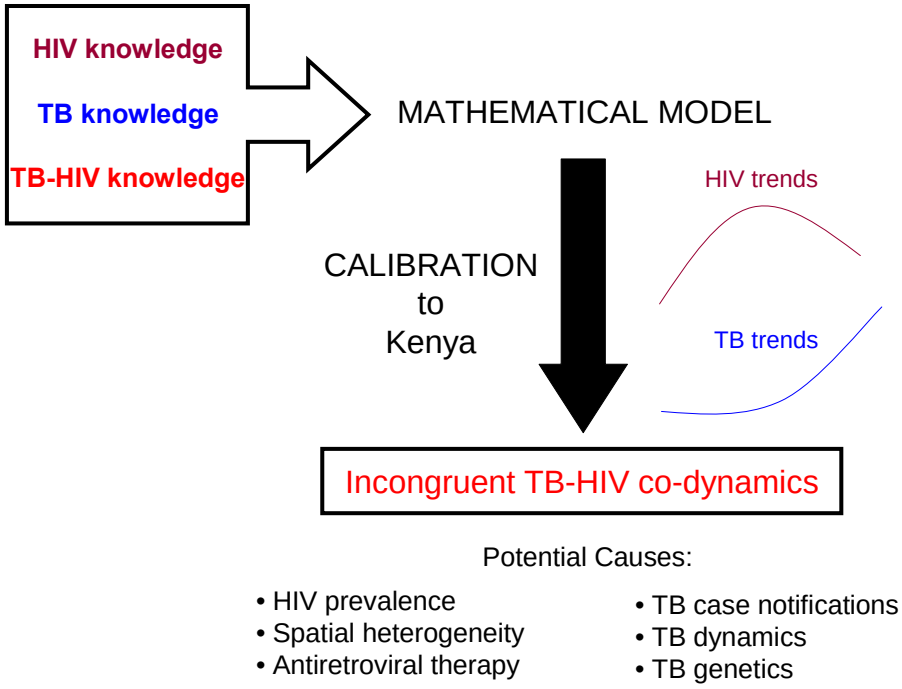

Note: We contrasted HIV and TB trends reported for Kenya by integrating person-level information for both diseases in a mathematical model and calibrating the model to country-level TB and TB-HIV measures spanning the period 1980-2004. The model cannot reconcile the substantial rise in TB numbers in light of the decreasing HIV numbers. We discuss potential causes for the reported discrepancies.

Fig. S2. TB-HIV model diagrams. A) TB transmission, treatment, and mortality in an HIV-free population were represented by progression through 42 categories. B) In an HIV infected population, HIV incidence, progression, and mortality is accounted by 5 stages. C) Details of the TB reinfection flow from the 'fully recovered HIV+ stage III'. This pattern applies to all other HIV stages. Each HIV stage includes the 42 TB categories for a total of 210 combined TB/HIV categories (Table S1).

A

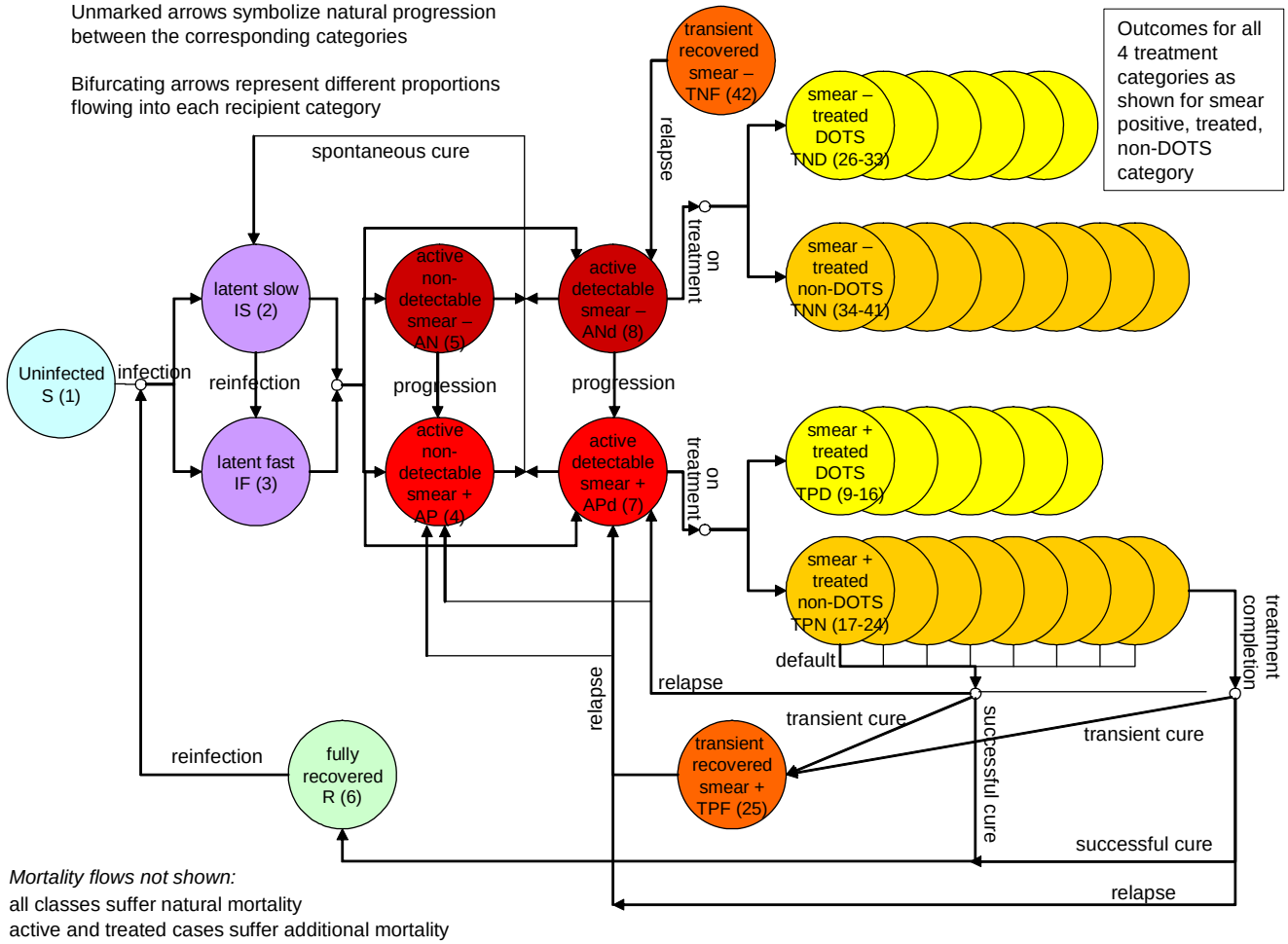

B

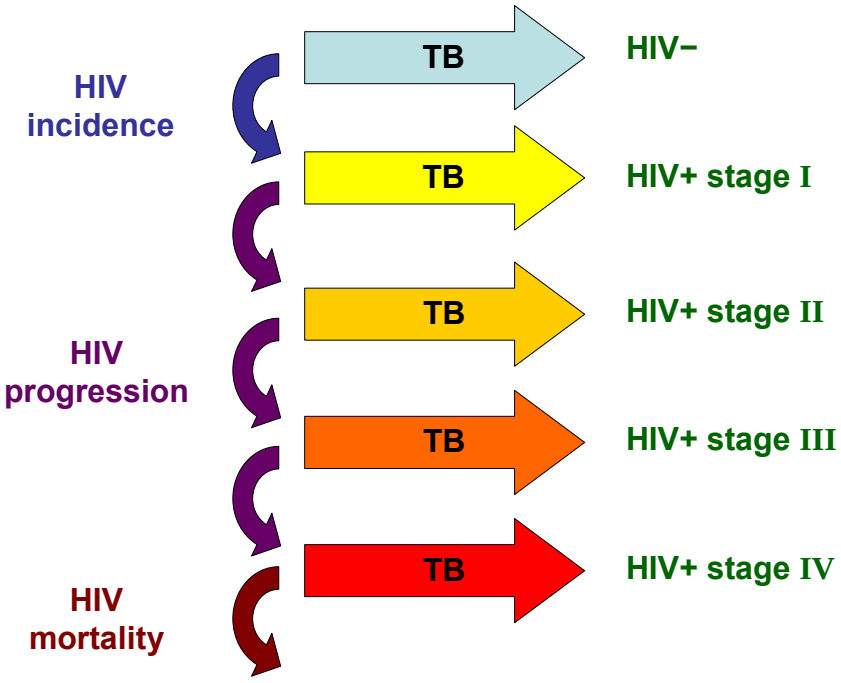
HIV
incidence
HIV
progression
HIV
mortality
TB
TB
TB
TB
TB
HIV−
HIV+ stage I
HIV+ stage II
HIV+ stage III
HIV+ stage IV

C

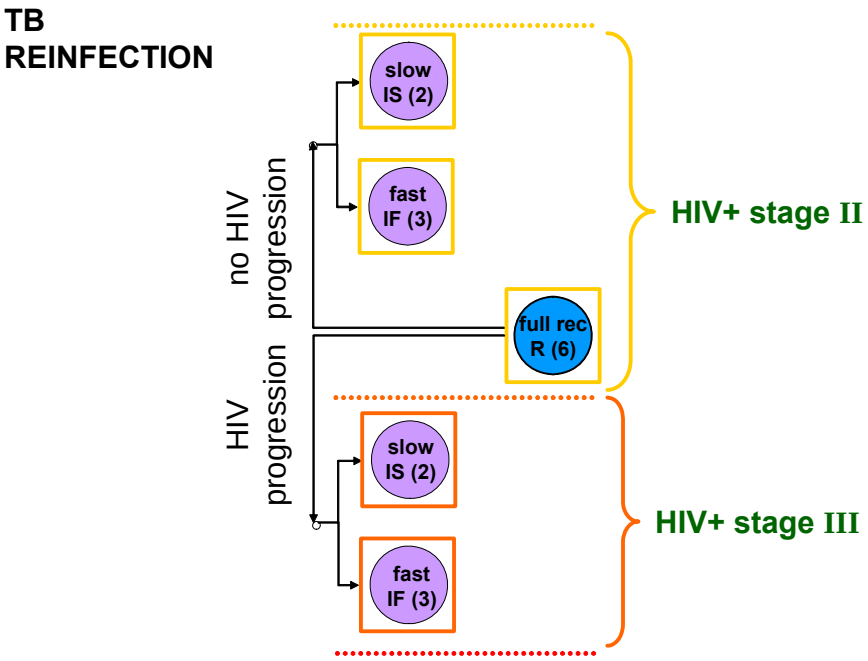
TB
REINFECTION
slow
IS (2)
fast
IF (3)
full rec
R (6)
no HIV progression
HIV progression
HIV+ stage II
slow
IS (2)
fast
IF (3)
HIV+ stage III

Fig. S3. Historical reconstruction of HIV prevalence following trends reported by Cheluget *et al.*[24] and TB treatment options in Kenya.

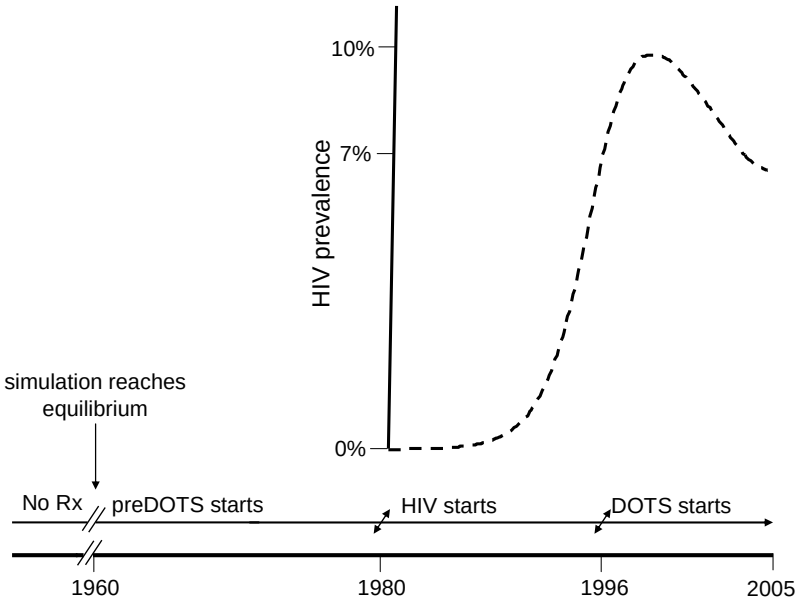

Note: Each simulation ran from a virgin epidemic until equilibrium, at which point we assumed conditions for the year 1960 were reached.

Fig. S4. Reported TB case notifications for Kenya and model output calibrated to various TB and joint TB-HIV measures reported for the period 1980-2004, following a monotonically increasing HIV epidemic that reaches a prevalence of 22.7% in 2005.